05,03

Photoluminescence related to dislocations in silicon plastically deformed under bending mode of central symmetry

© V.V. Emtsev, N.A. Sobolev, G.A. Oganesyan, A.E. Kalyadin, V.V. Toporov, D.S. Poloskin, A.M. Malyarenko

Ioffe Institute,
St. Petersburg, Russia

E-mail: emtsev@mail.ioffe.ru

Received May 21, 2025
Revised May 21, 2025
Accepted May 22, 2025

The photoluminescence related to dislocation formation in silicon wafers subjected to the bending mode of central symmetry by a circular male die, which has never been used for this purpose before, is investigated. An original technique whose efficiency was very recently demonstrated in the bending experiments on silicon wafers allows one to simultaneously determine the mechanical stress on the stretched and compressed sides of a wafer by the shift of the $520.5\,\mathrm{cm}^{-1}$ band in the Raman spectra. Plastic deformation of the wafer under mechanical loading is carried out at $T = 700\,^{\circ}\mathrm{C}$ for one hour. It is shown that all four known dislocation luminescence bands (lines *D1*–*D4*) and extended structural defects {113} appear on the stretched side of the wafer outside the central part. On the compressed side of the wafer outside the central part, lines *D3* and *D4* are clearly visible, as well as the edge luminescence line, but lines *D1* and *D2* are absent. When approaching the center of the wafer the *D3* and *D4* lines prevail on the stretched and compressed sides with residual deformation, and the *D4* line dominates in the very center. In this way, some prominent changes in the dislocation luminescence of plastically deformed silicon wafers under tensile and compressive stresses produced by the bending mode of central symmetry are evident.

Keywords: silicon, bending mode of central symmetry, plastic deformation, photoluminescence.

DOI: 10.61011/PSS.2025.05.61488.135-25

1. Introduction

It is known that silicon does not belong to the class of direct-gap semiconductors and in consequence has a low efficiency of radiative recombination of charge carriers. The efficiency of radiative recombination in silicon is several orders of magnitude lower than in direct-gap semiconductor materials. Nevertheless, a rapid development of silicon LEDs with a wavelength of $\sim 1.5\,\mu$m, which are important for the integration of microelectronic and optical components, remains an urgent technical task [1]. Various approaches are used to improve the radiative properties of silicon, one of which is based on the formation of extended structural defects in the material, such as dislocations. Photoluminescence related to the presence of dislocations was first observed in silicon wafers [2,3] deformed by the four-point bending method at $T = 850\,^{\circ}\mathrm{C}$ (often after preliminary scratching with a diamond needle). Four characteristic bands associated with dislocations were found in photoluminescence spectra in plastically deformed Si, among them lines *D1* (0.812 eV), *D2* (0.875 eV), *D3* (0.934 eV) and *D4* (1.000 eV). Further studies of dislocation luminescence, including on polycrystalline silicon, allowed one to conclude that the *D3* and *D4* lines form a pair, while the *D1* and *D2* lines are not a pair, but have different origins [4]. The intensity of these lines proved to be proportional to the dislocation density [2]. It is worth mentioning that the *D1*–*D4* dislocation lines in the photoluminescence spectrum turned out to be resistant to degradation upon heating above room temperature [5]. On the other hand, the intensity of these lines displays a strong quenching effect going from cryogenic to room temperature. This presents the main impediment to the practical use of dislocation luminescence. In the manufacture of LEDs on silicon, the *D1* line displaying higher thermal stability [5] is of great interest, since it corresponds to the transparency window of fiber optics. Making use of various technological methods while producing silicon-based structures it has been possible to observe this line even at room temperature [6]. One additional feature needs to be recognized. An increase in the dislocation density is tied to a redistribution of the intensity of the dislocation luminescence spectrum in the region of the *D1* line. In lieu of a relatively narrow line *D1* (with a half-width of 5–10 meV), a wide band (with a half-width of about 80 meV) consisting of several unresolved lines makes its appearance. It is generally accepted that the *D1* band covers a spectral range of 750–850 meV. The shape of the band in question depends on the crystal growth technique. In actual fact, the most intense region of dislocation luminescence in silicon grown by the floating zone technique falls on the long-wave wing of the *D1* band. On the contrary, in silicon crystals grown by the Czochralski technique the short-wave wing of the *D1* band is much more pronounced [7,8]. Moreover, the dislocation density also affects changes in the shape of dislocation luminescence spectra. At a relatively low dislocation density of $N_D \approx 10^6\,\mathrm{cm}^{-2}$, the *D1* and *D2* bands with a half-width of about 5 meV at cryogenic temperatures turned

out to be dominant in the spectrum [5]. Together with this, a significant increase in the dislocation concentration ($N_D \geq 10^8\,cm^{-2}$) strengthens the role of oxygen impurity in silicon crystals also changing the shape of the dislocation luminescence band. At low oxygen concentrations of $O_i \approx 10^{16}\,cm^{-3}$, the long-wave wing of the *D1* band is more pronounced, while in crystals with high oxygen concentrations of $[O_i] \approx 10^{18}\,cm^{-3}$, the maximum of this band is shifted to the short-wave range.

Although lengthy investigations of extended structural defects responsible for dislocation photoluminescence in silicon, reliable detailed information on their atomic structure is still poor. Together with such extended defects like various types of dislocations, plastic deformation of silicon can also give rise to the formation of other extended structural defects, among them the so-called rodlike defects, also specified by the {113} defects. These stacking faults turned out to be responsible for the band with a wavelength of $\sim 1.37\,\mu m$ in the luminescence spectrum [9]. Their atomic structure has not yet been reliably established, despite various model concepts discussed in the literature; see, for instance, [10–12].

As noted above, the formation of dislocation luminescence centers in silicon is strongly affected by oxygen impurity. First of all, this holds true for crystals grown by the Czochralski technique. Thermal annealing of oxygen-rich silicon samples triggers oxygen aggregation processes and, thus, forms oxygen precipitates that interact with dislocations. Under certain conditions, this makes possible producing light-emitting structures with *D1* line luminescence at room temperature which is basically compatible with the industrial technology of manufacturing integrated circuits [13–15]. On the other hand, dislocations decorated by oxygen precipitates may also present as effective centers of nonradiative recombination [16,17]. It is worth mentioning, however, that the issues related to dislocation luminescence in silicon are still pressing and require further experiments, including those without effects of oxygen impurity. To cite an example, it has recently been shown that the intense *D1* line in photoluminescence spectra can be observed just in the presence of „pure' dislocations (without oxygen precipitates) [18].

This article presents the results of a comparative study of dislocation luminescence spectra observed on the compressed and stretched sides of silicon wafers after high-temperature plastic deformation. A new element of such experiments is the use of the mode bending of central symmetry applying to silicon wafers by a circular male die, which has never been used before for dislocation formation. This makes possible increasing the mechanical stress on silicon wafers during deformation by an order of magnitude as compared with the known four-probe bending method. In addition, the original technique used in the present experiments allows one to simultaneously evaluate the mechanical stress on the stretched and compressed sides of the wafer under study during mechanical loading.

2. Experimental

The objects of the study were nearly circular silicon wafers with a diameter of $\sim 40\,mm$ and a thickness of 0.4 mm, polished on both sides. Wafers with the (111) surface orientation were cut from an n-type silicon crystal grown by the Czochralski technique (Cz–Si). The concentration of dissolved oxygen was $9.3 \cdot 10^{17}\,cm^{-3}$. The crystal was lightly doped with phosphorus whose concentration didn't exceed $1 \cdot 10^{14}\,cm^{-3}$.

In this work the experimental technique previously described in [19–21] was used. Wafers were placed on an annular pedestal with diameter of 18 mm and then subjected to the bending mode of central symmetry by a circular male die with diameter of 6 mm in the loading setup [22]. With this mechanical loading scheme, the silicon wafer is stretched on one side and compressed on the other.

Spectra were recorded making use of the Raman scattering technique based on an automated double grating monochromator DFS-24 with a Hamamatsu R943-02 photomultiplier tube, which was cooled to $T = -40\,^{\circ}C$ and operated in the photon counting mode. The spectral resolution was $\sim 2.2\,cm^{-1}$. Raman scattering spectra were excited by radiation from a solid-state yttrium aluminum garnet laser with wavelength of 532 nm (2.32 eV) and power of 40 mW. All spectra were recorded in a range from 470 to $540\,cm^{-1}$. The frequency calibration of the spectrometer was carried out using a mercury lamp against a spectral line of 546.072 nm. The error in determining the optical phonon frequency did not exceed $\pm 0.1\,cm^{-1}$. The radiation power of the emission incident onto a test wafer was ~ 30 mW, with the emission intensity being around $1\,kW/cm^2$. Under these conditions, there was no noticeable local heating of the wafer. Spectrum measurements at room temperature were carried out in the backscattering geometry. Raman spectra were recorded in the initial state (prior to loading) and after applying mechanical stresses. In the latter case all spectra were simultaneously recorded both from the frontal surface of a test wafer (the stretched side) and its backside surface (the compressed side). The magnitude of the mechanical stress applied on the both sides of the test wafer can be inferred from the frequency shift of a characteristic phonon line at $520.5\,cm^{-1}$. Any shift of this line allows calculating the magnitude of the mechanical stress applied to the test wafer. Let us take a brief look at how such calculations can be done.

It is known that in Raman spectra recorded on silicon under mechanical stress the bands associated with the phonon modes of the crystal lattice exhibit a shift and splitting. The triply degenerate branches of optical phonons F_{2g} are split into a singlet and a doublet. It must be emphasized that for the backscattering of light from the (111) surface both vibration modes, namely, the longitudinal (singlet) and transverse (doublet) ones, are present. For the scattering geometry $z(xy)\bar{z}$ being used in our case, the singlet is absent and only the doublet makes its appearance; see, for instance, [20]. Then, the frequency shift of the characteristic

phonon line in Raman spectra under the bending considered is determined from the equation

$$\Delta\omega_d = \frac{2(S_{11}+2S_{12})(p+2q)\sigma + S_{44}\sigma r}{6\omega_0}, \qquad (1)$$

where $\omega_0 = 520.5\,\mathrm{cm}^{-1}$ (optical phonon frequency); $p = -1.43\omega_0^2$, $q = -1.89\omega_0^2$, $r = -0.59\omega_0^2$ (anharmonic parameters); $S_{11} = 7.68 \cdot 10^{-12}\,\mathrm{Pa}^{-1}$, $S_{12} = -2.14 \cdot 10^{-12}\,\mathrm{Pa}^{-1}$, $S_{44} = 12.7 \cdot 10^{-12}\,\mathrm{Pa}^{-1}$ (elastic compliance constants in silicon at $T = 300\,\mathrm{K}$ [23–26]). On the stretched side of a test wafer under the bending conditions used in our experiments, for mechanical stress of $\sigma = 1.0\,\mathrm{GPa}$ the calculated shift of the transverse mode from the Si(111) surface was found to be

$$\Delta\omega_d = -3.72\,\mathrm{cm}^{-1}. \qquad (1a)$$

Then, on the compressed side of a test wafer the shift of this phonon line in Raman spectra another equation is valid [20]

$$\Delta\omega_h = \frac{\sigma(p+2q)(S_{11}+2S_{12})}{3\omega_0}, \qquad (2)$$

where $\Delta\omega_h$ is the frequency shift of the line under mechanical compression. In doing so, the calculated frequency shift of the characteristic phonon line under compressive stress of $\sigma = 1.0\,\mathrm{GPa}$ is equal to

$$\Delta\omega_h = 3.07\,\mathrm{cm}^{-1}. \qquad (2a)$$

These frequency shifts of the characteristic phonon line brought about by mechanical stresses due to stretching (1a) and compression (2a) were used as the reference values for evaluation in the present work. As depicted in Figure 1, a prominent effect of line shifting due to mechanical stress applied to the test wafer which was then subjected to plastic deformation. As already indicated above, the phonon lines can be simultaneously recorded on both sides of a silicon wafer, both prior to and after mechanical loading.

Under our experimental conditions, the frequency shift for the stretched side is $1.06\,\mathrm{cm}^{-1}$, which corresponds to mechanical stress of 0.28 GPa. For the compressed side, the phonon frequency shift of $1.17\,\mathrm{cm}^{-1}$ is achieved at a mechanical stress of 0.38 GPa. It is worth noting that the values given above refer to the most elastic deformation of the wafer being attainable in the present experiments. For the formation of extended structural defects like dislocations in the test wafer, its plastic deformation at higher temperatures is required. In our case, the plastic deformation of the test wafer under the mechanical loading occurred in a dry nitrogen atmosphere at $T = 700\,^\circ\mathrm{C}$ for one hour. Grasp, the mechanical stress during the high-temperature plastic deformation of the silicon wafer becomes less than that in the course of elastic deformation alone, but a quantitative assessment of this change is unfeasible under our experimental conditions. As a result of such high-temperature plastic deformation, the stretched side of the silicon wafer got convex, and the compressed side got concave. Both surfaces of the plastically deformed wafer are shown in Figure 2.

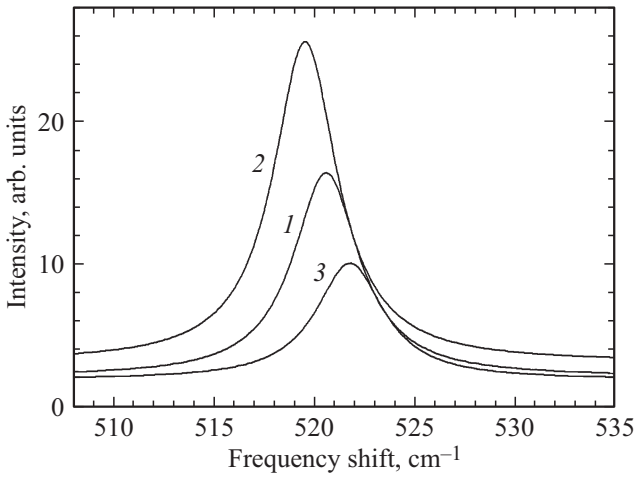

Figure 1. Frequency shifts of the characteristic phonon line for the silicon wafer under elastic stretching and compressive stresses. The line before mechanical loading is curve *1*; the line on the stretched side of the wafer is curve *2*; the line on the compressed side of the wafer is curve *3*.

Again, to determine residual stresses after the high-temperature deformation is possible by measuring shifts of the characteristic phonon line. The residual mechanical stresses at the central part of the deformed wafer were found to be 0.08 and 0.16 GPa on the stretched (convex) and compressed (concave) sides of the wafer, respectively.

The formation of dislocations and other extended structural defects in the plastically deformed plate was then studied by means of photoluminescence. Luminescence was excited by a laser with wavelength of $\lambda = 532\,\mathrm{nm}$ and power of up to 40 mW. Photoluminescence spectra were recorded with the aid of an MDR-23 monochromator and an AlGaAs photodiode operating at room temperature. The resolution of the optical setup was 5 nm.

3. Results and discussion

3.1. Wafer after plastic deformation under stretching

On the stretched side of the wafer, at the spot that was outside the annular support (see Figure 2, *a*, spot *6*), in the luminescence spectrum shown in Figure 3, all four lines *D1* to *D4* related to the formation of dislocations are clearly visible, together with the characteristic line, associated with the appearance of extended stacking faults known in the literature as the {113} structural defects.

The most intense dislocation line in the spectrum turned out to be tied with the *D4* line. We believe that the left wing of the *D1* line is associated with oxygen precipitates. Where the silicon wafer comes into contact with the annular support during the high-temperature plastic deformation (Figure 2, *a*, spot *5*), the intensity of all four lines in

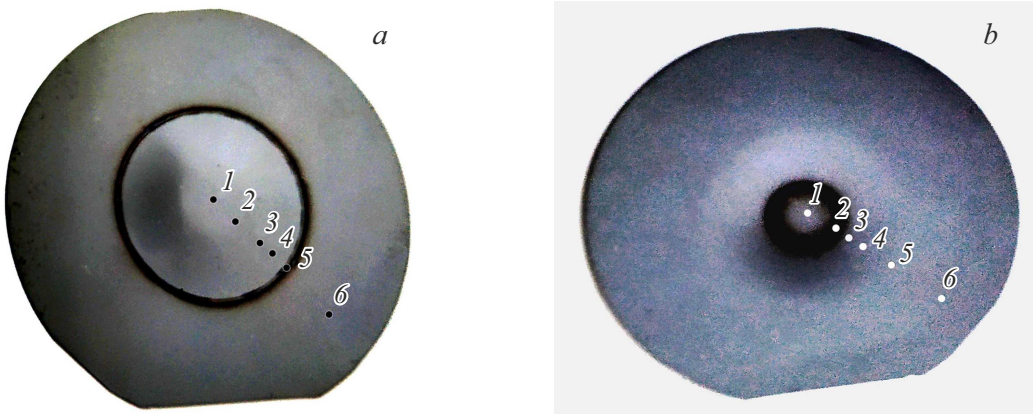

Figure 2. Surfaces of the silicon wafer after high-temperature plastic deformation under stretching (*a*) and compression (*b*). The spots at which photoluminescence spectra were taken are designated by spots of *1* to *6*.

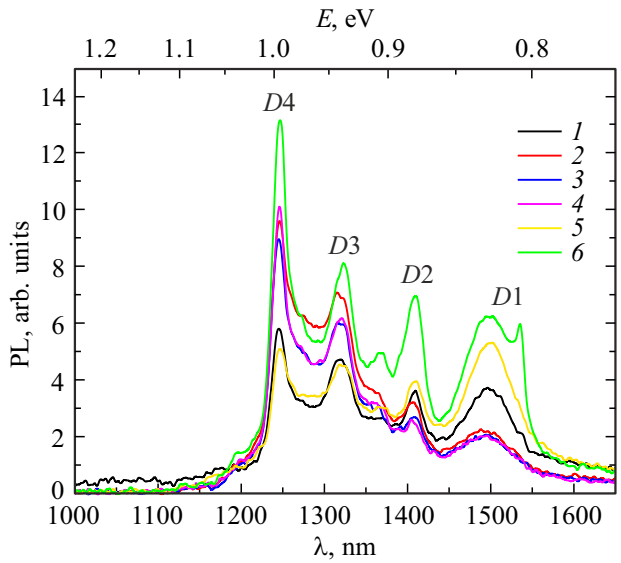

Figure 3. Photoluminescence spectra recorded at different spots on the silicon wafer after the high-temperature plastic deformation under stretching. The spots at which the spectra were recorded are designated by numbers from *1* to *6* (see Figure 2, *a*).

the photoluminescence spectrum shown in Figure 3 drops significantly and the shape of the lines changes somewhat as compared to the spectrum taken on the plateau at spot *6*; see above. As we approach the center of the plastically deformed wafer (Figure 2, *a*, spots $4 \rightarrow 2$), the *D3* and *D4* lines noticeably predominate in the luminescence spectrum shown in Figure 3. At the very center of the wafer subjected to the high-temperature plastic deformation (Figure 2, *a*, spot *1*), a sizeable decrease in the intensity of all the lines in the photoluminescence spectrum is observed leaving the *D4* line to be dominant; see Figure 3. In addition, the shape of the spectrum in the range of the line *D1* allows one to believe that this line is actually absent, and the nearest broad band is associated with the formation of precipitates.

3.2. Wafer after plastic deformation under compression

On the compressed side of the silicon wafer, at the spot that was outside the annular support (see Figure 2, *b*, spot *6*), in the photoluminescence spectrum shown in Figure 4, the *D3* and *D4* lines are clearly seen, together with the characteristic line associated with the edge luminescence.

However, the lines *D1* and *D2* are not seen in the spectrum. At the spot where the wafer came into contact with the annular support during the high-temperature plastic deformation (Figure 2, *b*, spot *5*), the photoluminescence spectrum shown in Figure 4 retains the general appearance of the lines that are present, but their intensity falls off. To cite an example, the intensity of the edge luminescence line drops nearly by five times, and the intensity of the lines *D3* and *D4* decreases by one and a half times. As we approach the central part of the wafer (Figure 2, *b*, spots $4 \rightarrow 3$), the intensity of the lines *D3* and *D4* in the photoluminescence spectrum changes only slightly; see Figure 4. However, already upon contact between the annular support and the wafer (Figure 2, *b*, spot *2*), all four lines *D1* to *D4* are reliably recorded in the luminescence spectrum shown in Figure 4. The same conclusion can be made regarding the spectrum taken at the very center of the wafer plastically deformed under compression (Figure 2, *b*, spot *1*): in the luminescence spectrum shown in Figure 4, the intensity of the lines *D3* and *D4* increases slightly, leaving the other two lines almost unchanged.

3.3. Effects of temperature measurements and pump power on the luminescence spectra

As an illustration, Figure 5 shows the photoluminescence spectra recorded at the very center of the wafer after the high-temperature plastic deformation under compression (Figure 2, *b*, spot *1*).

In the photoluminescence spectrum measured at $T = 10$ K all four lines *D1* to *D4* are clearly visible; see Figure 5. Quenching effects upon the intensity of the luminescence lines associated with dislocations start immediately with an increase in the temperature of measurements to $T = 30$ K. As can be seen from this figure, with a rise in the temperature of measurements the intensity of all luminescence lines in the spectra decreases sharply and a significant broadening of these lines is observed. The line

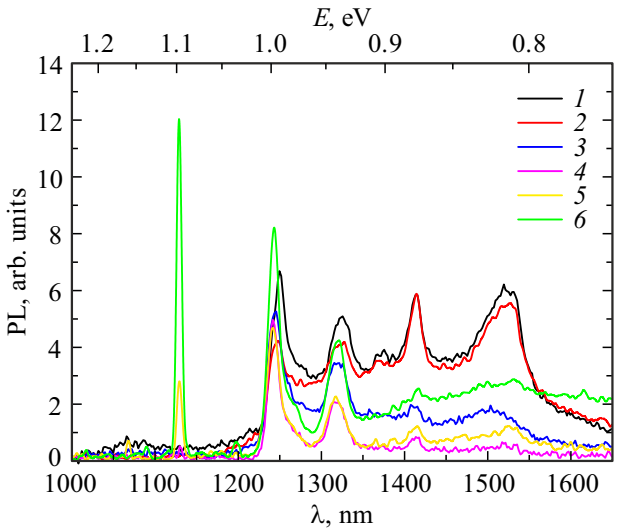

Figure 4. Photoluminescence spectra recorded at different spots on the silicon wafer after the high-temperature plastic deformation under compression. The spots at which the spectra were recorded are designated by numbers from *1* to *6* (see Figure 2, *b*). The order in which the dislocation lines appear in the photoluminescence spectra see Figure 3.

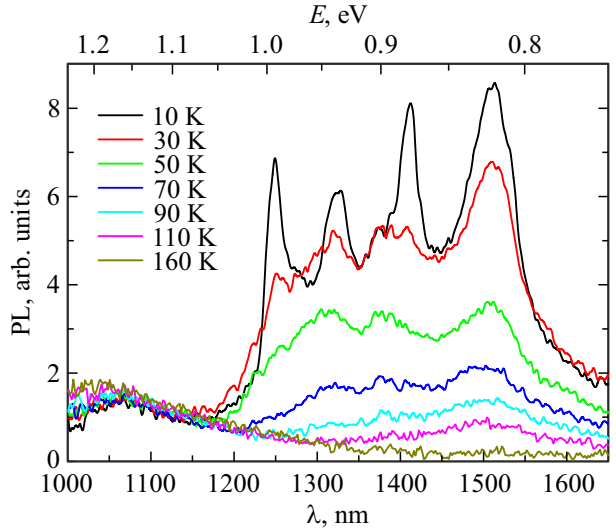

Figure 5. Effects of photoluminescence spectra upon temperature of measurements. Spectra were taking at the center of the silicon wafer after the high-temperature plastic deformation under compression. Spot *6*, at which the spectra were recorded; see Figure 2, *b*. The order in which the dislocation lines appear in the photoluminescence spectra see Figure 3.

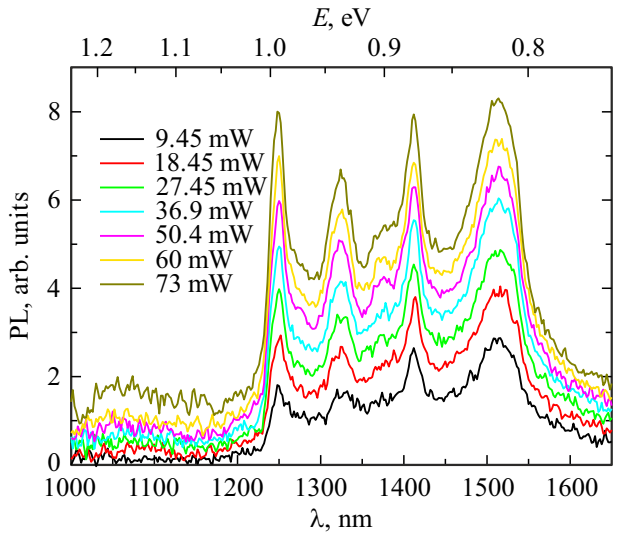

Figure 6. Effects of the pump power on photoluminescence spectra taken at the center of the silicon wafer after the high-temperature plastic deformation under compression. The temperature of measurements is $T = 10$ K. Spot *6* at which the spectra were recorded; see Figure 2, *b*. The order in which the dislocation lines appear in the photoluminescence spectra see Figure 3.

D4 disappears faster than the other ones and this is also true for similar silicon wafers with dislocations produced by different technological methods [13]. In actual fact, the lines *D2* to *D4* lose gradually their original shape. With a further rise in the temperature of measurements to $T = 50$ K a progressive degradation of the luminescence spectra is going on, so only line *D1* can be identified with some degree of certainty; see Figure 5. The photoluminescence spectra at $T \geq 70$ K generally appear to be uninformative.

Of interest is also effects of the pump power on the photoluminescence spectra associated with dislocations. As an example, Figure 6 shows the luminescence spectra taken at $T = 10$ K at the very center of the silicon wafer after the high-temperature plastic deformation under compression (Figure 2, *b*, spot *1*).

Already at the minimal pump power of 9.45 mW, all four lines *D1* to *D4* make their appearance in the photoluminescence spectrum. As the pump power increases up to 73 mW, the positions of all lines remain unchanged and their intensity increases sharply, but the ratio of the line intensities is kept nearly constant. In addition, with the maximum pump power it is also possible to observe the line at $\sim 1.37\,\mu$m associated with the presence of extended stacking faults marked the {113} structural defects.

4. Conclusions

In this paper we studied the photoluminescence spectra related to the formation of dislocations and other extended structural defects in silicon. The silicon wafers were subjected to high-temperature plastic deformation under

the bending mode of central symmetry. This method of introducing extended structural defects into silicon under mechanical stretching and compression has not been used before. Thus, studying the photoluminescence spectra associated with the presence of dislocations in silicon wafers allowed one to get a searching look at the characteristic features of their formation due to high-temperature plastic deformation under stretching and compression conditions. For both stretched and compressed sides of the test wafer, it turns out that the line *D4* is dominant in the luminescence spectrum taken at the very center of the wafer. Its intensity increases significantly with increasing pump power. Along with the line *D4*, for the stretched side of the silicon wafer subjected to the high-temperature plastic deformation, the presence of extended stacking faults known as the {113} structural defects was detected in the luminescence spectra, too. It is interesting that on the compressed side of the plastically deformed silicon wafer, outside its contact with the annular support during the high-temperature plastic deformation, two strong lines *D3* and *D4* are make their appearance in the photoluminescence spectra, together with the characteristic line associated with the edge luminescence. Marked changes in the intensity of all lines associated with dislocations and other extended structural defects introduced in different parts of the plastically deformed silicon wafer, were also noted.

Conflict of interest

The authors declare that they have no known competing interests.

References

[1] N. Margalit, C. Xiang, S.M. Bowers, A. Bjorlin, R. Blum, J.E. Bowers. Appl. Phys. Lett. **118**, 220501 (2021). https://doi.org/10.1063/5.0050117

[2] N.A. Sobolev, A.E. Kalyadin, O.V. Feklisova, E.B. Yakimov. Semiconductors **55**, 633 (2021). https://doi.org/10.1134/S1063782621070174

[3] N.A. Drozdov, A.A. Patrin, V.D. Tkachev. JETP Lett. **23**, 597 (1976).

[4] M. Reiche, M. Kittler. Crystals **6** (7), 74 (2016). https://doi.org/10.3390/cryst6070074

[5] E.A. Steinman. Physics of the Solid State **47**, 5 (2005). https://doi.org/10.1134/1.1853432

[6] N.A. Sobolev, A.E. Kalyadin, K.F. Shtel'makh, P.N. Aruev, V.V. Zabrodskiy, E.I. Shek. Semiconductors **57**, 283 (2023). DOI: 10.61011/SC.2023.04.56427.4810

[7] E.A. Steinman, V.V. Kveder, V.I. Vdovin, H.G. Grimmeiss. Solid State Phenomena **69–70**, 23 (1999). https://doi.org/10.4028/www.scientific.net/SSP.69-70.23

[8] S. Pizzini, M. Guzzi, E. Grilli, G. Borionetti. Journal of Physics: Condensed Matter **12**, 10131 (2000). https://doi.org/10.1088/0953-8984/12/49/312

[9] A.E. Kalyadin, K.F. Shtel'makh, P.N. Aruev, V.V. Zabrodski, K.V. Karabeshkin, E.I. Shek, N.A. Sobolev. Semiconductors **54**, 687 (2020). https://doi.org/10.1134/S1063782620060081

[10] S. Takeda. Jpn. J. Appl. Phys. **30**, L639 (1991). https://doi.org/10.1143/JJAP.30.L639

[11] L.I. Fedina, A.K. Gutakovskii, A.V. Latyshev, A.L. Aseev. In: Advances in Semiconductor Nanostructures, Growth, Characterization, Properties and Applications, ed by A. Latyshev, A. Dvurechenskii, A. Aseev (Elsevier, Amsterdam, 2016) p. 383.

[12] L. Jeyanathan, E.C. Lightowlers, V. Higgs, G. Davies. Mater. Sci. Forum **143–147**, 1499 (1994). https://doi.org/10.4028/www.scientific.net/MSF.143-147.1499

[13] S. Binetti, S. Pizzini, E. Leoni, R. Somaschini, A. Castaldini, A. Cavallini. J. Appl. Phys. **92**, 2437 (2002). https://doi.org/10.1063/1.1497450

[14] K. Bothe, R.J. Falster, J.D. Murphy. Appl. Phys. Lett. **101**, 032107 (2012). https://doi.org/10.1063/1.4737175

[15] S. Binetti, R. Somaschini, A. LeDonne, E. Leoni, S. Pizzini, D. Li, D. Yang. J. Phys.: Condens. Matter **14**, 13247 (2002). https://doi.org/10.1088/0953-8984/14/48/375

[16] N.A. Sobolev, A.E. Kalyadin, K.F. Shtel'makh, E.I. Shek, V.I. Sakharov, I.T. Serenkov. Semiconductors **56**, 390 (2022). DOI: 10.21883/SC.2022.06.53535.9832

[17] A. Borghesi, B. Pivac, A. Sassella, A. Stella. J. Appl. Phys. **77**, 4169 (1995). https://doi.org/10.1063/1.359479

[18] V.I. Vdovin, L.I. Fedina, A.K. Gutakovskii, A.E. Kalyadin, E.I. Shek, K.F. Shtel'makh, N.A. Sobolev. Crystallography Reports **66**, 625 (2021). DOI: 10.1134/s1063774521040210

[19] G.A. Oganesyan, I.I. Novak. Journal of Surface Investigation, X-ray, Synchrotron and Neutron Techniques **3**, 962 (2009). https://doi.org/10.1134/S1027451009060202

[20] I.I. Novak, V.V. Baptizmanskii, L.V. Zhoga. Opt. Spectrosc. **43**, 145 (1977).

[21] I.I. Novak, G.A. Oganesyan. Journal of Surface Investigation, X-ray, Synchrotron and Neutron Techniques **1**, 294 (2007). https://doi.org/10.1134/S1027451007030111

[22] V.V. Emtsev, V.V. Toporov, G.A. Oganesyan, A.A. Lebedev, D.S. Poloskin. Physica B: Condensed Matter **684**, 415949 (2024). https://doi.org/10.1016/j.physb.2024.415949

[23] E. Anastassakis, A. Pinczuk, E. Burstein, F.H. Pollak, M. Cardona. Solid State Communications **8**, 133 (1970). https://doi.org/10.1016/0038-1098(70)90588-0

[24] I.D. Wolf. Semicond. Sci. Technol. **11**, 139 (1990). https://doi.org/10.1088/0268-1242/11/2/001

[25] V. Poborchii, T. Tada, T. Kanayama. Appl. Phys. Lett. **97**, 041915 (2010). https://doi.org/10.1063/1.3474604

[26] A. Gassenq, S. Tardif, K. Guilloy, I. Duchemin, N. Pauc, J.M. Hartmann, D. Rouchon, J. Widiez, Y.M. Niquet, L. Milord, T. Zabel, H. Sigg, J. Faist, A. Chelnokov, F. Rieutord, V. Reboud, V. Calvo. J. Appl. Phys. **121**, 055702 (2017). https://doi.org/10.1063/1.4974202